Supporting Information: Optimizing nitroxide biradicals for Cross-Effect MAS-DNP: the role of g-tensors' distance

Frédéric Mentink-Vigier[a]

[a]National High Magnetic Field Laboratory, Florida State University, Tallahassee, FL, 32301, USA
Email: fmentink@magnet.fsu.edu

1. Hamiltonian

The MAS-DNP simulations use the same Hamiltonian described elsewhere.[1–4] The 3-spin systems are composed of two electrons and one proton $\{^1\text{H-e}_a\text{-e}_b\}$. In the µw rotating frame, the time-dependent Hamiltonian can be written as:

$$\begin{aligned}\hat{H}(t) &= \hat{H}_Z(t) + \hat{H}_{HF}(t) + \hat{H}_D(t) + \hat{H}_J + \hat{H}_d + \hat{H}_{\mu w} \\ &= \hat{H}_0(t) + \hat{H}_{\mu w}\end{aligned}$$

where

$$\hat{H}_Z(t) = \sum_n \sum_i \left(g_i(t)\beta_e B_0 - \omega_{\mu w}\right)\hat{S}_{z,i} + m_{I,i}A^N_{z,i}(t)\hat{S}_{z,i} - \omega_n \hat{I}_{z,n}$$

$$\hat{H}_{HF}(t) = \sum_i \{A_{z,i,n}(t)\hat{S}_{z,i}\hat{I}_{z,n} + 2(A^+_{i,n}(t)\hat{S}_{z,i}\hat{I}^+_n + A^-_{i,n}(t)\hat{S}_{z,i}\hat{I}^-_n)\}$$

$$\hat{H}_D(t) = \sum_{a,b} D_{a,b}(t)(2\hat{S}_{z,\mathrm{a}}\hat{S}_{z,\mathrm{b}} - 1/2(\hat{S}^+_a\hat{S}^-_b + \hat{S}^-_a\hat{S}^+_b))$$

$$\hat{H}_J = \sum_{a,b} -2J_{a,b}(\hat{S}_{z,a}\hat{S}_{z,b} + 1/2(\hat{S}^+_a\hat{S}^-_b + \hat{S}^-_a\hat{S}^+_b))$$

$$\hat{H}_d(t) = \sum_{n,n'} d_{n,n'}(t)(2\hat{I}_{z,\mathrm{a}}\hat{I}_{z,\mathrm{b}} - 1/2(\hat{I}^+_a\hat{I}^-_b + \hat{I}^-_a\hat{I}^+_b))$$

$$\hat{H}_{\mu w} = \sum_i \omega_{1,s}\hat{S}_{x,i}$$

where g_i is the g-tensor value for electron i, $\omega_{\mu w}$ the µw irradiation frequency, $A^N_{z,i}$ the secular part of the hyperfine interaction between electron i and ^{14}N that bears the radical, ω_n the nuclear Larmor frequency, $A_{i,n}$ the hyperfine coupling between electron i and nucleus n, $D_{a,b}$ the dipolar coupling between electrons a and b, and $J_{a,b}$ the exchange interaction between electrons a and b (the two radical moieties, respectively), $d_{n,n'}$ is the dipolar coupling between nuclei n and n'. The µw Rabi frequency, $\omega_1/2\pi$, is assumed to be small and is treated as a perturbation. Evolution superoperators are calculated as described in detail in ref. [2]. The nuclear polarization enhancements are then calculated as

$$\varepsilon\ (Nt_r) = {Tr(\rho(Nt_\mathrm{r})\hat{I}_z)}\Big/{Tr(\rho(0)\hat{I}_z)}$$

The effect of moderate dipolar/J exchange interaction splitting has been accounted for in the μw rotor-events. Using the definitions presented in reference [5], only the microwave off-resonance has been modified. For electron a or b the frequency offset becomes

$$\Delta\omega_{a/b} = \omega_{a/b} - \omega_{\mu\mathrm{w}} + m_s^{a/b} \times (D_{a,b} - J_{a,b})$$

Where $\omega_{a/b}$ is the Zeeman frequency, $\omega_{\mu w}$ is the microwave frequency and $(D_{a,b} - J_{a,b})$ is the z component of the dipolar/exchange interaction. The splitting is reproduced by choosing randomly, for each electron and each crystal orientation, m_s = + ½ or – ½. The approach is valid for dipolar/exchange interactions that are ~1/10 of the EPR linewidth and for temperature/field giving moderate electron polarization (<10 %).

2. Illustration of $|P_a\text{-}P_b|$

Figure S1 reports the quasi periodic steady state electron and nuclear polarization for a three-spin system: electrons a and b with nucleus n. The maximum electron polarization difference represented in figure S1, $|\mathrm{P_a} - \mathrm{P_b}|_{\max}$ is the

uniform (or infinite) norm of the function $f(t) = (P_a(t) - P_b(t))$on the segment $[t,t+\tau_r]$ representing one steady-state rotor-period (τ_r): $||\mathrm{P_a} - \mathrm{P_b}||_\infty = |\mathrm{P_a} - \mathrm{P_b}|_{\max}$. When the nuclear relaxation time is very long, the nuclear relaxation follows the relation:[2,6,7] $||\mathrm{P}_a - \mathrm{P}_b||_\infty = |P_n|$

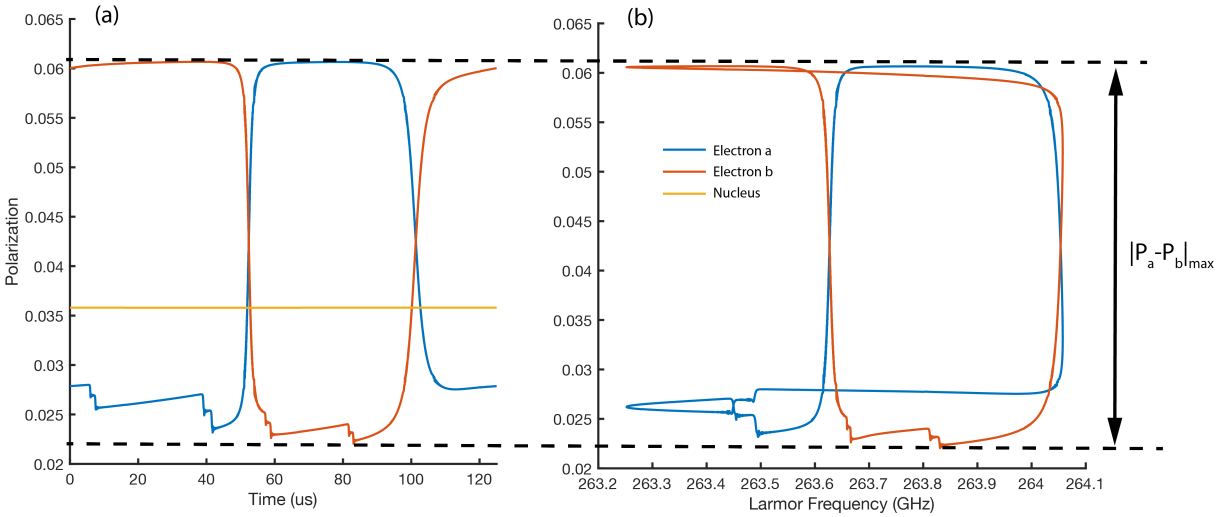

Fig S1: Quasi-periodic steady state polarization obtained under microwave irradiation. Figure (a) represents the electron a,b and nuclear polarizations time evolution for one rotor period after 30 s. (b), same as (a) except electron *a,b* polarization are represented against electron *a*'s Larmor frequency. Dotted line represents the maximum electron polarization's difference $|\mathrm{P_a} - \mathrm{P_b}|_{\max}$

3. Determination of the optimal J for the idealized model

To carry out the simulations with the idealized model, the exchange interaction optimized in the range of 1 to 30 MHz to find the simulation conditions leading to optimal polarization gain $|\epsilon_B|$. This is reported in figure S2. The optimal gain is reached for $J_{\mathrm{a,b}}$ = 20 MHz.

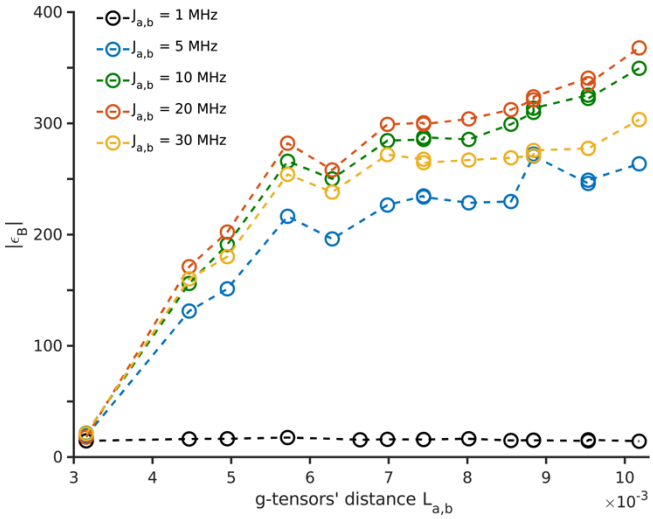

Fig S2: Evolution of $|\epsilon_B|$ in the idealized case as a function of $L_{a,b}$, black circles, $J_{a,b}$ = 1 MHz, blue circles, $J_{a,b}$ = 5 MHz, green circles, $J_{a,b}$ = 10 MHz, red circles, $J_{a,b}$ = 20 MHz and yellow circles, $J_{a,b}$ = 30 MHz. For these simulations, the powder average was obtained with 400 single crystal orientations REPULSION grid.[8]

4. Optimal Field position

Figure S2 reports the optimal magnetic field position for the idealized and realistic case reported in the main text.

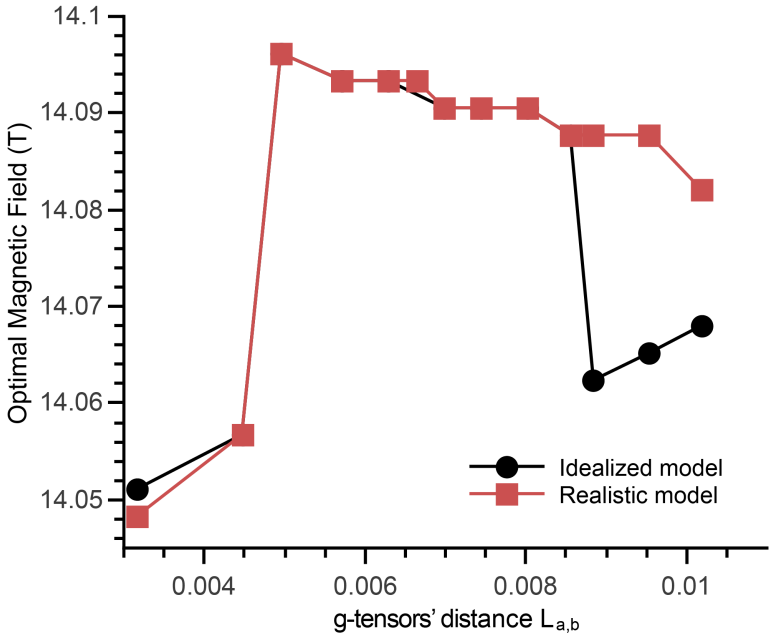

Fig. S3: Value of the optimal field position for the idealized spin system in figure 2 and realistic in figure 5.

5. Effect of $T_{1,e}$ and Magnetic field on $|\epsilon_B|$

Using the "box model" with realistic parameters, the polarization gain has been computed for different magnetic field and electron relaxation times. The results show identical trends in figure S4.

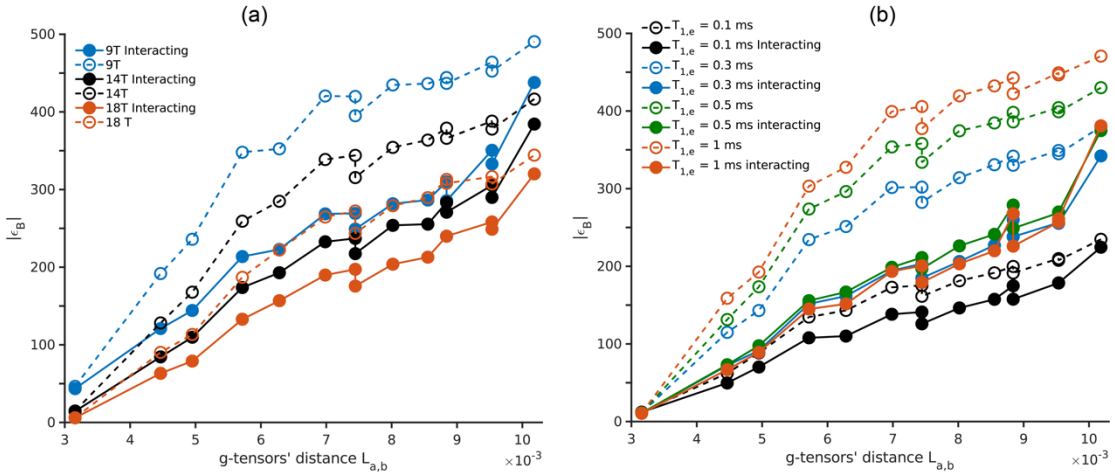

Fig S4: Evolution of $|\epsilon_B|$ in the idealized case as a function of $L_{a,b}$ for (a) different main magnetic field, black 9.4 T, blue 14.1 T, red 18.8 T, (b) for different T_{1e} values, black 0.1 ms, blue 0.3 ms, green 0.5 ms, red 1 ms (at 14.1 T). Dotted line corresponds to the isolated three-spin system and the full line corresponds to the interacting BOX model. For these simulations, the powder average was obtained with 400 single crystal orientations REPULSION grid.[8]

References

1 F. Mentink-Vigier, U. Akbey, Y. Hovav, S. Vega, H. Oschkinat and A. Feintuch, Fast passage dynamic nuclear polarization on rotating solids, *J. Magn. Reson.*, 2012, **224**, 13–21.

2 F. Mentink-Vigier, U. Akbey, H. Oschkinat, S. Vega and A. Feintuch, Theoretical aspects of Magic Angle Spinning - Dynamic Nuclear Polarization, *J. Magn. Reson.*, 2015, **258**, 102–120.

3 F. Mentink-Vigier, S. Paul, D. Lee, A. Feintuch, S. Hediger, S. Vega and G. De Paepe, Nuclear depolarization and

absolute sensitivity in magic-angle spinning cross effect dynamic nuclear polarization, *Phys. Chem. Chem. Phys.*, 2015, **17**, 21824–21836.

4 F. Mentink-Vigier, G. Mathies, Y. Liu, A. L. Barra, M. A. Caporini, D. Lee, S. Hediger, R. G. Griffin and G. De Paepe, Efficient cross-effect dynamic nuclear polarization without depolarization in high-resolution MAS NMR, *Chem. Sci.*, 2017, **8**, 8150–8163.

5 F. Mentink-Vigier, S. Vega and G. De Paepe, Fast and accurate MAS–DNP simulations of large spin ensembles, *Phys. Chem. Chem. Phys.*, 2017, **19**, 3506–3522.

6 K. Kundu, F. Mentink-Vigier, A. Feintuch and S. Vega, *DNP Mechanisms*, WILEY-VCH Verlag GmbH & Co. KGaA, eMagRes., 2019, vol. 8.

7 S. Hediger, D. Lee, F. Mentink-Vigier and G. De Paëpe, *MAS-DNP Enhancements : Hyperpolarization, Depolarization, and Absolute Sensitivity*, WILEY-VCH Verlag, eMagRes., 2018, vol. 7.

8 M. Bak and N. C. Nielsen, REPULSION, A Novel Approach to Efficient Powder Averaging in Solid-State NMR, *J. Magn. Reson.*, 1997, **125**, 132–139.